Localized flow control by photothermal actuation of pNIPAAm hydrogel brushes in a macroporous silicon membrane

Youngsik Song, Nafis Mustakim, Mayank Pandey and Sang-Woo Seo

Department of Electrical Engineering,

The City College of New York,

160 Convent Avenue,

New York, NY 10031, USA

Email: swseo@ccny.cuny.edu

Abstract

We present the control of liquid flow through arrayed micron-sized pores in a macroporous silicon membrane. The pores are coated with about 150 nm polymer N-isopropylacrylamide (pNIPAAm) hydrogel brushes and 200 nm polypyrrole layer, which works as photothermal actuator. The size of pore openings is controlled by utilizing the swelling and de-swelling behavior of temperature-sensitive pNIPAAm brushes, and the temperature on pNIPAAm brushes is changed by 815 nm near infra-red(NIR) illumination to polypyrrole photothermal element layer. The dimension change of the pore openings is investigated by observing the transmitted light and fluorescence signal intensity through the pores in the membrane while changing the ambient temperature. It has shown that the intensity of transmitted light can be controlled by adjusting the ambient temperature manipulation across the low critical solution temperature (LCST) of the hydrogel brushes. The localized control of liquid flow through the pores is demonstrated by the diffusion of fluorescein dye from the bottom of the membrane to the surface of the membrane using pulsed NIR light illumination. Fast dynamic response of fluorescein dye diffusion upon the illumination of NIR light suggests that the presented photothermal actuation approach could be applied to diverse biomedical applications such as a localized drug release system.

Keywords: pNIPAAm, hydrogel, atomic transfer radical polymerization, photothermal actuation,

1 Introduction

Hydrogels are cross-linked porous polymers that can change their shape and volume upon exposure to external stimuli such as temperature, pH, pressure, magnetic field, etc. (Ahmed 2015) Owing to these environment-responsive nature, hydrogels have attracted great interest over the last few decades to be utilized as active elements in drug release, tissue engineering, microfluidic systems, cell culture to name a few.(Vasani, McInnes et al. 2011; Nagase, Yamato et al. 2018; Tan, Lin et al. 2020) Among the stimuli-responsive hydrogels, thermo-responsive poly N-isopropylacrylamide(pNIPAAm) hydrogel is of great interest in bio-related applications because the phase transition temperature (also known as lower critical solution temperature, LCST) is very close to human body temperature and the LCST can be readily adjusted by the copolymerization with acrylamide(AAm) based monomers as well as biocompatibility.(Liu, Fraylich et al. 2009; Cooperstein and Canavan 2013; Chatterjee, Hui et al. 2018) There are increasing efforts to incorporate thermo-responsive pNIPAAm hydrogel to bio related microfluidic systems utilizing swelling and de-swelling behavior upon exposure to temperature change to realize microvalves.(Tan, Lin et al. 2020; Wang, Toyoda et al. 2020) Hydrogel microvalve structures have been demonstrated using ultraviolet(UV) polymerization(Beebe, Moore et al. 2000; Tan, Lin et al. 2020; Wang, Toyoda et al. 2020), molding(Sugiura, Hirama et al. 2015; Li, Motschman et al. 2020; Su, Chuah et al. 2021), and 3-D printing(Mansoorifar, Tahayeri et al. 2020; Lan, Shang et al. 2021; Mannel, Weigel et al. 2021) methods for diverse design and operation strategies. However, the miniaturization of such microvalves in microfluidic systems is challenging and limited to several hundreds of micrometer ranges due to the fundamental obstacles in the mentioned-processes such as indirect proximity contact and scattering in UV polymerization technique.

The development of atom transfer radical polymerization(ATRP) technique has paved ways to synthesize polymers in controlled manners. (Wang and Matyjaszewski 1995) Further development of surface initiated ATRP(SI-ATRP) process enables to modify the functionality of a surface by directly anchoring *smart* polymers on the surface of diverse structures as a layer of polymer brushes for variety of applications including drug delivery, microfluidic channels, cell culture, anti-biofouling, tissue engineering, separation to name a few.(Zhou, Zhu et al. 2007; Zhang, Finlay et al. 2009; Zhu, Zhang et al. 2013; Zhang and Chiao 2015; Nagase, Yamato et al. 2018) Among the SI-ATRP methods, more controllable method to create *smart* functional surface is grafted-from approach. In grafted-from approach, the polymerization starts from the covalently bonded immobilized initiators on the surface, and this approach enables to synthesize a robust polymer brush layer on a surface for a specific functionality by proper selection of monomers, ligands, initiators, solvents and polymerization environment. (Kim, Schmitt et al. 2015)

By combining thermo-responsive pNIPAAm hydrogel and the grafted-from SI-ATRP approach, unique functional systems for biomedical applications have been demonstrated. (Morsch, Schofield et al. 2010; Vasani, McInnes et al. 2011; Pan, Guo et al. 2013; Szuwarzynski, Zaraska et al. 2013; Nagase, Yamato et al. 2018) When the ambient temperature is near the LCST of the pNIPAAm, the pNIPAAm hydrogel brushes are being collapsed(de-swelled) and become hydrophobic mushroom shape structure due to intramolecular hydrogen bonding. On the other hand, when the ambient temperature is below the LCST, the pNIPAAm hydrogel brushes are being hydrophilic brush shape structure (swelled) and extended up to 3 times longer in length compared to collapsed(de-swelled) state due to intermolecular hydrogen bonding. (Li, Xie et al. 2009; Yu, Kieviet et al. 2015)

Localized heat generation by the photothermal effect by illuminating near field infra-red(NIR) light at a specific location is one of the simplest and well developed heat generation method in biomedical applications.(He, Frueh et al. 2016; Raza, Hayat et al. 2019; Sun, Huang et al. 2020) There are wide varieties of NIR light absorbing materials including metallic and metal oxide nanostructures, organic and inorganic nanomaterials.(Jaque, Maestro et al. 2014; Jung, Verwilst et al. 2018; Frueh, Rutkowski et al. 2022) Among the photothermal heating materials, polypyrrole(PPy) is a unique heat generation element because it has strong absorption behavior to wide IR wavelength range with high potothermal conversion efficiency and biocompatibility which make versatile usage especially in biomedical application.(Kim, Kim et al. 2017)

In this paper, we create three-dimensional arrayed micro fluidic valves by devising macroporous silicon structure with layered pNIPAAm brushes and PPy, and demonstrate the control of liquid flow through micro channels by utilizing the physical phase transition behavior of pNIPAAm brushes through localized NIR-induced photothermal actuation.

2 Experimental

N-isopropylacrylamide (NIPAAm), 2-bromoisobutyryl bromide (BIBB, 98%), aminopropyl triethoxysilane (APTES, 98%), N, N, N', N'', N''- pentamethyldiethylene-triamine (PMDETA), Pyrrole(C_4H_5N) and Fe (III) sulfonate were purchased from TCI, USA. Copper(II) Bromide ($CuBr_2$) was purchased from Strem Chemicals, USA. Ascorbic acid ($C_6H_8O_6$) and Triethylamine(TEA) was purchased from VWR, USA. EDTA titrant (0.1 N) was purchased from Aqua Solutions, USA. They were used as received without further purification. Deionized(DI) water (Reagent Grade, Electron Microscopy Sciences, Inc., USA) was used for all aqueous solutions.

2.1 Polymerization of N-isopropylacrylamide for hydrogel brushes

The substrates used for the grafting of NIPAAm were glass slide, p-type silicon(Si) wafer with 100 nm thick silicon dioxide(SiO_2) and macroporous p-type Si membrane with 1 μm thick silicon dioxide (SiO_2) layer along the pore walls. A layer of pNIPAAm hydrogel brushes on the SiO_2 surface was formed based on the oxygen tolerant SI-ATRP method.(Varma, Bureau et al. 2016)

The substrates were sonicated in acetone for 10 min. and rinsed with acetone, methanol, and isopropyl alcohol followed by nitrogen (N_2) dry. The solvent-cleaned substrates were immersed in the freshly mixed Piranha solution (3:1 H_2SO_4: H_2O_2) at room temperature for 30 min. for the silanol(-OH) functionalization. After silanol functionalization, substrates were immersed in 2 vol. % APTES in degassed toluene for the silane(-NH_2) functionalization for 20 min. followed by brief sonication in Toluene to remove physisorbed silane molecules from the SiO_2 surface, and rinsed with toluene and ethanol. The silane functionalized substrates were baked in an oven at 110 °C for 30 min. Next, the substrates were immersed in 1 vol. % TEA in degassed toluene, and then 1 % (in volume) BIBB was added drop-wisely at room temperature. The substrates were kept in the solution for 2 hours in N_2 ambient with stirring, and rinsed with toluene and ethanol followed by N_2 dry.

pNIPAAm hydrogel brushes were grafted by SI-ATRP process of NIPAAm at room temperature. The polymerization process was carried out in a glove bag in N_2 ambient. In a two neck round bottom flask with 10 mL degassed water, 0.5 g NIPAAm was added and dissolved with a magnetic stirrer. After complete dissolution of NIPAAm, 1.5 mg of $CuBr_2$, 20 μL of PMDETA, and 15 mg of ascorbic acid were added successively. After complete dissolution, the

magnetic stirrer was removed from the solution, and the BIBB initiator functionalized substrate was placed in the flask. The necks were sealed with septum and the polymerization process was continued in the glove bag for 18 hours. Finally, the pNIPAAm grafted substrates were rinsed with EDTA titrant and DI water.

2.2 Polymerization of Pyrrole

Pyrrole was polymerized by vapor phase polymerization (VPP) method using Fe(III) sulfonate as an initiator.(Winther-Jensen, Chen et al. 2004) A substrate was cleaned by sonication in acetone for 10 min. followed by rinsing with acetone, methanol and isopropyl alcohol. After drying with N_2, the solvent cleaned substrate was dip coated in 5 wt. % Fe (III) sulfonate in butanol for 1 min. and excessive Fe (III) sulfonate solution on the surface was blown by a stream of N_2. After drying, the substrate was placed vertically on a custom made substrate mount in a vacuum desiccator, and 25 μL of pyrrole droplet was placed on a cover glass 1 cm below the substrate. Once the desiccator was evacuated down to ~ 1 mTorr, the vacuum valve was closed, and the VPP was carried out for 2 hours. VPP of Pyrrole on pNIPAAm hydrogel brushes was carried out by the same procedures except sonication and solvent cleaning steps.

2.3 Preparation of a macroporous silicon membrane

Periodically arranged, one-side opened macroporous Si wafer was purchased from Smart Membranes, Germany. The detailed processes to create through-hole Si membrane was described in the previous publication. (Song, Azmand et al. 2020) Briefly, the one side opened macroporous

Si wafer was attached on a lapping mount using a wax, and two step lapping procedure was carried out successively using two types of slurry solutions containing 1 μm alumina powders for initial lapping and 0.25 μm alumina powders for fine lapping. After creating through hole pores by the lapping, pores were enlarged by repeated thermal-oxidation and buffered oxide etching processes to obtain 400 μm thick macroporous Si membrane with 7 μm pore openings in diameter and 1 μm thick silicon dioxide(SiO_2) layer along the pore walls.

3 Result and discussion

3.1 pNIPAAm Hydrogel Brush

Fig. 1 shows the optical images of SiO_2/Si wafers with different thicknesses of pNIPAAm brush layer. The thickness of the dried pNIPAAm brush layer measured by ellipsometry is around 150 nm after 18 hours of polymerization time. The adhesion test based on the American Society for Testing and Materials (ASTM) D3359-17 method shows that the adhesion between dried pNIPAAm hydrogel brushes and SiO_2 surface was very strong.

It is well known that the LCST of pure pNIPAAm hydrogel is around 32 °C, and there is a reversible transition in opaqueness near the LCST.(Liu, Fraylich et al. 2009) To investigate the opaqueness transition of the thin pNIPAAm brush layer, the transmission characteristics of 150 nm thick pNIPAAm brush layer on a glass slide was measured by UV-Vis spectroscopy. The glass slide with pNIPAAm hydrogel brushes was placed in a DI water filled cuvette with a custom made substrate mount, and UV-Vis spectra in the range of 330 nm to 850 nm with the resolution of 1.3 nm were obtained by a F20-UV spectrometer (Filmetrics, San Diego, CA 92121, USA). Fig. 1(e)

shows the transmitted light characteristics through the pNIPAAm brush layer on the glass substrate at 24 °C and 38 °C. There is about 5% decrease in transmitted light intensity over the wavelength range when the water temperature is raised above the LCST, but the decrement is not as significant as the 1 mm thick bulk pNIPAAm hydrogel which showed about 90 % decrease in transmission due to the very thin layer of pNIPAAm brushes. (Song, Azmand et al. 2020)

3.2 Transmission through a macroporous silicon membrane with pNIPAAm brushes

We characterized the temperature response of pNIPAAm brushes polymerized on pore walls by observing light transmission through the Si macroporous membrane over ambient temperature change. The pNIPAAm brushes were synthesized similarly as the NIPAAm polymerization processes on planar SiO_2/Si wafers and glass slides with extra process steps of brief sonication for removing trapped air and complete filling of liquid reactants into pores. The expected length of pNIPAAm brushes on pore walls is around 150 nm since all the preparation and polymerization processes were almost identical as the processes on the planar SiO_2 surface.

A microscope was customized to measure transmitted light through pores in the macroporous Si membrane. Fig.2 (a) shows a schematic diagram of the transmission characterization setup. The light transmission through pores was measured by illuminating white light from the bottom of the microscope while changing the ambient temperature of water in a heat chamber. A custom-made aluminum chamber connected to a digital temperature controller with two openings sealed with cover glasses for light paths shown in the inset was used to mount the macroporous Si membrane. The light transmission through pores was recorded as a video format by a digital microscope camera, and the transmitted light intensity is calculated from the captured

images using ImageJ software (National Institute of Health). (Schneider, Rasband et al. 2012; Schindelin, Rueden et al. 2015) Fig. 2(b) shows the change of transmitted light intensity as a function of ambient water temperature. The transmitted light intensity shows a gradual transition over the measured temperature range which is strongly related to the area of pore openings. When the ambient temperature is approaching to the LCST, the pNIPAAm hydrogel brushes are starting to collapse, the pore openings are enlarged and more light transmission is allowed. Meanwhile, as ambient temperature is approaching to room temperature, the pNIPAAm hydrogel brushes are being extended, the pore openings are reduced, and light transmission is reduced. Interestingly, the transition of transmission of light through pores near the LCST is not as sharp as the direct light transmission through a bulk hydrogel. (Song, Azmand et al. 2020) It implies that the structural transition between extended structure and mushroom structure of pNIPAAm brushes responding to the temperature change is not as fast as the opaqueness change of the bulk pNIPAAm hydrogel.

3. 3 Polypyrrole characterization

Polypyrrole (PPy) was synthesized from pyrrole by vapor phase polymerization(VPP) method using Fe (III) sulfonate as an initiator. There are several deposition techniques to functionalize a surface with the initiator. We found that deep coating in Fe (III) sulfonate followed by dry with a stream of N_2 was the most effective technique to obtain a uniform and smooth PPy layer on a surface. The thickness of the PPy layer was measured by a surface profilometer (DekTak 150, Veeco Instrument Inc., Plainview, NY 11803) at the stylus force of 1 mg over a groove created by a Teflon needle. The typical thickness of the PPy layer obtained by VPP method was about 200

nm. for 2 hr. VPP process. Fig. 3(a) shows the UV-Vis spectra of the PPy layer on a glass substrate. The absorbance of broad-band light by the thin PPy layer occurs over the wide wavelength range. Fig. 3(b) and (c) show the photothermal characteristics of the PPy layer on glass and on pNIPAAm hydrogel brushes by illuminating NIR light at 815 nm with various powers in air. The temperature at the surface was recorded by a FLIR i7 (FLIR system, USA) compact IR thermal imaging camera. The temperature change by the photothermal effect from the PPy layer shows initial rapid increase followed by gradual saturation with illumination time. The highest temperature observed at the same illumination power is slightly higher from PPy layer on a glass substrate than the temperature observed from PPy layer on pNIPAAm hydrogel brush layer.

3.5 Photothermal actuation of pNIPAAm hydrogel brush by PPy in a macroporous Si membrane

To demonstrate the photothermal actuation of pNIPAAm brushes by PPy at a specific local area, the measurement setup used previously for light transmission measurement was modified to illuminate NIR light to the top of a macroporous membrane using a dichroic mirror as shown in the Fig. 4(a).

Fig. 4 (b) shows the normalized transmitted light intensity as a function of time while pulses of NIR light with different powers are illuminated for 2 sec. of ON with 3 sec. of OFF period. (Supplemental Material, Video 1) The transmission of light through pores are responding to the repeated NIR light illumination due to the physical structural transition of pNIPAAm brushes between mushroom to extended brush structures. The higher transmitted light intensities were observed with higher NIR light illumination power as expected which demonstrates the higher degree of collapse of hydrogel brushes responding to the higher NIR light power. However,

the transmitted light intensities don't reach to the maximum within 2 sec. illuminations, which imply that the temperature doesn't reach to the LCST of pNIPAAm brushes to be fully collapsed.

Fig. 4(c) shows the transmitted light intensity by varying the illumination time at 90 mW NIR light illumination. The NIR light illumination times were 2, 4, 6 and 8 sec. and the OFF time was 10 sec. The incremental rates of transmitted light intensity are similar for 4 different illumination times, and the higher transmitted light intensity was observed from longer illumination time as expected.

Fig. 4(d) shows the background temperature dependent transmitted light intensity change as a function of time. The temperature of ambient water in the aluminum chamber was pre adjusted by the temperature controller before measuring transmission of light. The background temperatures were 27 °C(blue), 29 °C(pink) and 32 °C(red), and the NIR light ON time was 2 sec. and the OFF time was 3 sec. at 90 mW of NIR power. When the background temperature was set at 32 °C, the change of transmitted light intensity by photohermal actuation is very small since the hydrogel brushes were already in near-full collapsed state, and the thermo-response of hydrogel brushes is minimal as shown in Fig. 2(b). When the background temperatures were 27 °C and 29 °C, the transmitted light intensities are responding to the illumination of NIR light due to the structural transition of hydrogel brushes by the photothermal actuation. The initial transmitted light intensities before NIR light illumination are similar for both temperatures which implies similar degrees of collapse of hydrogel brushes. When the NIR light is turned on, the increase of transmitted light intensity at 29 °C background temperature increases more than the transmitted light intensity at 27 °C background temperature because the change rate of transmission to temperature is higher at 29 °C than that of at 27 °C which is related the collapse rate of hydrogel brushes, and the different response to the background temperature indicates that the degree of

collapse of pNIPAAm brushes is higher at higher temperature near the LCST. It is a good agreement to the thermo-response of pNIPAAm hydrogel brushes shown in Fig. 2 which shows steeper slope near the LCST.

The control of liquid flow through the micron sized pores in a macroporous Si membrane by localized light actuation was observed using the modified microscope setup to excite fluorescence signal from 2 wt.% fluorescein dye in water solution as shown in Fig. 5(a). The macroporous membrane is mounted in a 3-D printed chamber sealed by two fluoropolymer o-rings. The bottom chamber is connected to a fluorescein dye reservoir which allows maintaining constant dye concentration in the bottom chamber. The upper chamber is connected to a peristaltic pump which can flush water in the upper chamber. The inset shows the image of the 3-D printed chamber for the experimental setup. Before each measurement, the dye solution in the upper chamber was flushed with DI water until the fluorescence signal intensity becomes minimal. Once the fluorescence signal intensity reaches minimal, the pump was turned off to stop flushing and the diffusion of fluorescein dye from the bottom chamber to the upper chamber was measured with and without the NIR light illumination. The optical power of NIR light through the objective lens was measured at 90 mW.

Fig. 5(b) shows normalized cumulative fluorescence signal in the upper chamber by various NIR modulation schemes. Two slopes are observed from each NIR pulse modulation scheme. Without NIR light illumination, fluorescein dye diffuses from the bottom chamber to upper chamber through pores with slower diffusion rate which is expected through smaller sized pore openings formed by extended pNIPAAm brushes at room temperature shown as gentle slopes. When the NIR light is illuminated, pNIPAAm brushes are collapsed due to the photothermal heat generation from PPy, and pore openings are enlarged. Owing to the enlarged pore opening, the

diffusion of fluorescein dye from the bottom chamber to the upper chamber gets faster and slopes of fluorescence signal intensity increases, representing steep slopes(-). Again, when the NIR light illumination is stopped, the pNIPAAm brushes return to extended structure. As a result, pore openings become smaller and the diffusion rate is decreased, representing gentle slopes(-)

4 Conclusion

In summary, we have demonstrated the photothermal actuation of thermo-responsive pNIPAAm hydrogel brushes on the walls of the periodically arranged micron-sized pores in the Si macroporous membrane. The pNIPAAm brushes were grafted from the pore walls by the ATRP method, and PPy photothermal element was polymerized on pNIPAAm brushes. The photothermal actuation of pNIPAAm hydrogel brushes was achieved by illuminating NIR light onto polypyrrole layer, and photothermal actuation of pNIAPPm hydrogel brushes was observed by the transmitted light and diffusion of fluorescein dye through pores. It has been demonstrated that the physical structure of pNIPAAm brushes and the openings of pores were modulated by remote NIR light illumination. It was also found that the response of pNIPAAm brushes to structural deformation becomes faster near the LCST of pNIPAAM hydrogel. The demonstrated approach has potentials for the localized remote flow control in drug delivery system and bio-responsive actuators.

Acknowledgement

This work was supported by CUNY PSC-CUNY grant and National Science Foundation grant (NSF-1952469).

Author Contribution

Y. Song and S. Seo conceived the idea and designed the research. Y. Song, N. Mustakim, and P. Mayank performed the experiments. Y. Song, N. Mustakim, and S. Seo analyzed and interpreted the results. Y. Song drafted the manuscript and all authors contributed to the writing of the manuscript.

Declarations

Conflict of Interests The authors declare no competing interests.

References

Ahmed, E. M. (2015). "Hydrogel: Preparation, characterization, and applications: A review." Journal of Advanced Research **6**(2): 105-121.

Beebe, D. J., J. S. Moore, et al. (2000). "Functional hydrogel structures for autonomous flow control inside microfluidic channels." Nature **404**(6778): 588-+.

Chatterjee, S., P. C. L. Hui, et al. (2018). "Thermoresponsive Hydrogels and Their Biomedical Applications: Special Insight into Their Applications in Textile Based Transdermal Therapy." Polymers **10**(5).

Cooperstein, M. A. and H. E. Canavan (2013). "Assessment of cytotoxicity of (N-isopropyl acrylamide) and Poly(N-isopropyl acrylamide)-coated surfaces." Biointerphases **8**.

Frueh, J., S. Rutkowski, et al. (2022). "Propulsion Mechanisms of Light-Driven Plasmonic Colloidal Micromotors." Advanced Photonics Research **3**(1).

He, W. P., J. Frueh, et al. (2016). "Guidable GNR-Fe₃O₄-PEM@SiO₂ composite particles containing near infrared active nanocalorifiers for laser assisted tissue welding." Colloids and Surfaces a-Physicochemical and Engineering Aspects **511**: 73-81.

Jaque, D., L. M. Maestro, et al. (2014). "Nanoparticles for photothermal therapies." Nanoscale **6**(16): 9494-9530.

Jung, H. S., P. Verwilst, et al. (2018). "Organic molecule-based photothermal agents: an expanding photothermal therapy universe." Chemical Society Reviews **47**(7): 2280-2297.

Kim, H., K. Kim, et al. (2017). "Nature-inspired thermo-responsive multifunctional membrane adaptively hybridized with PNIPAm and PPy." Npg Asia Materials **9**.

Kim, M., S. K. Schmitt, et al. (2015). "From Self-Assembled Monolayers to Coatings: Advances in the Synthesis and Nanobio Applications of Polymer Brushes." Polymers **7**(7): 1346-1378.

Lan, D. X., Y. L. Shang, et al. (2021). "Facile Fabrication of Hollow Hydrogel Microfiber via 3D Printing-Assisted Microfluidics and Its Application as a Biomimetic Blood Capillary." Acs Biomaterials Science & Engineering **7**(10): 4971-4981.

Li, P. F., R. Xie, et al. (2009). "Thermo-responsive gating membranes with controllable length and density of poly(N-isopropylacrylamide) chains grafted by ATRP method." Journal of Membrane Science **337**(1-2): 310-317.

Li, Y., J. D. Motschman, et al. (2020). "Injection Molded Microfluidics for Establishing High-Density Single Cell Arrays in an Open Hydrogel Format." Analytical Chemistry **92**(3): 2794-2801.

Liu, R. X., M. Fraylich, et al. (2009). "Thermoresponsive copolymers: from fundamental studies to applications." Colloid and Polymer Science **287**(6): 627-643.

Mannel, M. J., N. Weigel, et al. (2021). "Combining Hydrophilic and Hydrophobic Materials in 3D Printing for Fabricating Microfluidic Devices with Spatial Wettability." Advanced Materials Technologies **6**(9).

Mansoorifar, A., A. Tahayeri, et al. (2020). "Bioinspired reconfiguration of 3D printed microfluidic hydrogels via automated manipulation of magnetic inks." Lab on a Chip **20**(10): 1713-1719.

Morsch, S., W. C. E. Schofield, et al. (2010). "Surface Actuation of Smart Nanoshutters." Langmuir **26**(14): 12342-12350.

Nagase, K., M. Yamato, et al. (2018). "Poly(N-isopropylacrylamide)-based thermoresponsive surfaces provide new types of biomedical applications." Biomaterials **153**: 27-48.

Pan, G. Q., Q. P. Guo, et al. (2013). "Thermo-Responsive Hydrogel Layers Imprinted with RGDS Peptide: A System for Harvesting Cell Sheets." Angewandte Chemie-International Edition **52**(27): 6907-6911.

Raza, A., U. Hayat, et al. (2019). "“Smart” materials-based near-infrared light-responsive drug delivery systems for cancer treatment: A review." Journal of Materials Research and Technology **8**(1): 1497-1509.

Schindelin, J., C. T. Rueden, et al. (2015). "The ImageJ ecosystem: An open platform for biomedical image analysis." Molecular Reproduction and Development **82**(7-8): 518-529.

Schneider, C. A., W. S. Rasband, et al. (2012). "NIH Image to ImageJ: 25 years of image analysis." Nature Methods **9**(7): 671-675.

Song, Y., H. R. Azmand, et al. (2020). "Rapid photothermal actuation of light-addressable, arrayed hydrogel columns in a macroporous silicon membrane." Sensors and Actuators a-Physical **301**.

Su, C. X., Y. J. Chuah, et al. (2021). "A Facile and Scalable Hydrogel Patterning Method for Microfluidic 3D Cell Culture and Spheroid-in-Gel Culture Array." Biosensors-Basel **11**(12).

Sugiura, Y., H. Hirama, et al. (2015). "Fabrication of Microfluidic Valves Using a Hydrogel Molding Method." Scientific Reports **5**.

Sun, P. F., T. Huang, et al. (2020). "Dynamic-Covalent Hydrogel with NIR-Triggered Drug Delivery for Localized Chemo-Photothermal Combination Therapy." Biomacromolecules **21**(2): 556-565.

Szuwarzynski, M., L. Zaraska, et al. (2013). "Pulsatile Releasing Platform of Nanocontainers Equipped with Thermally Responsive Polymeric Nanovalves." Chemistry of Materials **25**(3): 514-520.

Tan, J. W., H. S. Lin, et al. (2020). "A Stimuli-Responsive Hydrogel Array Fabrication Scheme for Large-Scale and Wearable Microfluidic Valving." Journal of Microelectromechanical Systems **29**(5): 1115-1117.

Varma, S., L. Bureau, et al. (2016). "The Conformation of Thermoresponsive Polymer Brushes Probed by Optical Reflectivity." Langmuir **32**(13): 3152-3163.

Vasani, R. B., S. J. P. McInnes, et al. (2011). "Stimulus-Responsiveness and Drug Release from Porous Silicon Films ATRP-Grafted with Poly(N-isopropylacrylamide)." Langmuir **27**(12): 7843-7853.

Wang, J. S. and K. Matyjaszewski (1995). "Controlled Living Radical Polymerization - Halogen Atom-Transfer Radical Polymerization Promoted by a Cu(I)Cu(II) Redox Process." Macromolecules **28**(23): 7901-7910.

Wang, Y. Z., K. Toyoda, et al. (2020). "A simple micro check valve using a photo-patterned hydrogel valve core." Sensors and Actuators a-Physical **304**.

Winther-Jensen, B., J. Chen, et al. (2004). "Vapor phase polymerization of pyrrole and thiophene using iron(III) sulfonates as oxidizing agents." Macromolecules **37**(16): 5930-5935.

Yu, Y. L., B. D. Kieviet, et al. (2015). "Stretching of collapsed polymers causes an enhanced dissipative response of PNIPAM brushes near their LCST." Soft Matter **11**(43): 8508-8516.

Zhang, H. B. and M. Chiao (2015). "Anti-fouling Coatings of Poly(dimethylsiloxane) Devices for Biological and Biomedical Applications." Journal of Medical and Biological Engineering **35**(2): 143-155.

Zhang, Z., J. A. Finlay, et al. (2009). "Polysulfobetaine-Grafted Surfaces as Environmentally Benign Ultralow Fouling Marine Coatings." Langmuir **25**(23): 13516-13521.

Zhou, Z. Y., S. M. Zhu, et al. (2007). "Grafting of thermo-responsive polymer inside mesoporous silica with large pore size using ATRP and investigation of its use in drug release." Journal of Materials Chemistry **17**(23): 2428-2433.

Zhu, Y. Z., F. Zhang, et al. (2013). "A novel zwitterionic polyelectrolyte grafted PVDF membrane for thoroughly separating oil from water with ultrahigh efficiency." Journal of Materials Chemistry A **1**(18): 5758-5765.

Figure Captions

Figure 1. Images of various thicknesses of pNIPAAm hydrogel brush layer (a) 20 nm pNIPAAm layer on SiO_2/Si wafer, (b) 85 nm pNIPAAm layer on SiO_2/Si wafer, (c) 150 nm pNIPAAm layer on SiO_2/Si wafer, (d) 150 nm pNIPAAm layer on a glass slide, and (e) UV-vis spectra of 150 nm pNIPAAm layer on a glass slide at 24 °C(blue) and 38 °C(red)

Figure 2. (a) Schematic diagram of the measurement setup for the optical transmission through the pNIPAAm brush polymerized on a macroporous silicon membrane, (b) Transmitted light intensity through a macroporous membrane between 25 °C and 37 °C

Figure 3. (a) Optical transmission through polypyrrole layer on a glass slide (green) and polypyrrole layer on a pNIPAAm brush/glass slide(blue), (b) Temperature response of polypyrrole layer on a glass slide with various powers of 815 nm NIR light illumination, (c) Temperature response of polypyrrole layer on a pNIPAAm brush/ glass slide with various powers of 815 nm NIR light illumination

Figure 4. (a) Schematic diagram of the measurement setup for the optical transmission through the pNIPAM brush polymerized on a macroporous silicon membrane for 815 nm NIR light illumination, (b) Transmitted light intensity through a macroporpus membrane with PPy/pNIPAAm brush layer with various powers of pulsed 815 nm NIR light illumination, (c) Transmitted light intensity through a macroporpus membrane with PPy/pNIPAAm brush layer with various 815 nm NIR light illumination time with 90 mW power, and (d) Transmitted light intensity through a macroporpus membrane with PPy/pNIPAAm brush layer with pulsed 90 mW power of 815 nm NIR light illumination with different background temperature 27 °C, 29 °C and 32 °C

Figure 5. (a) Schematic diagram of the measurement setup for the diffusion of fluorescein dye through the PPy/pNIPAAm brush layer deposited macroporous silicon membrane by 815 nm NIR illumination, (b) Normalized fluorescence signal from diffused fluorescein dye through the membrane with various NIR ON( )/OFF( ) duration

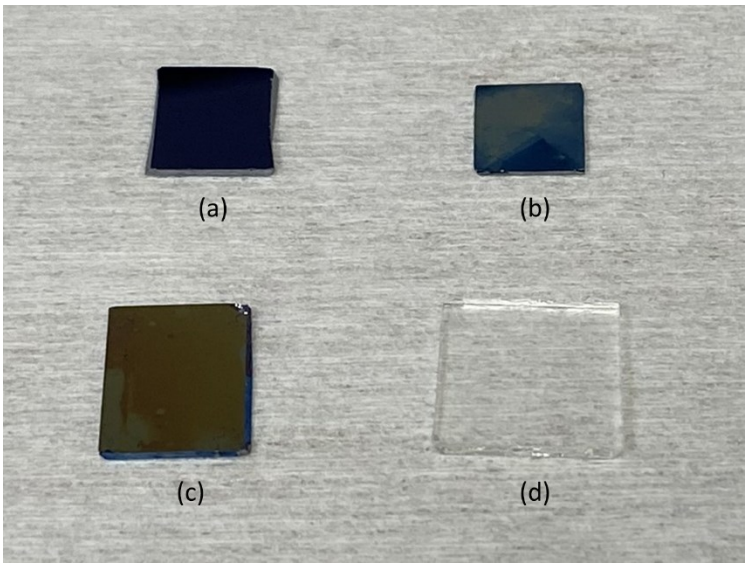

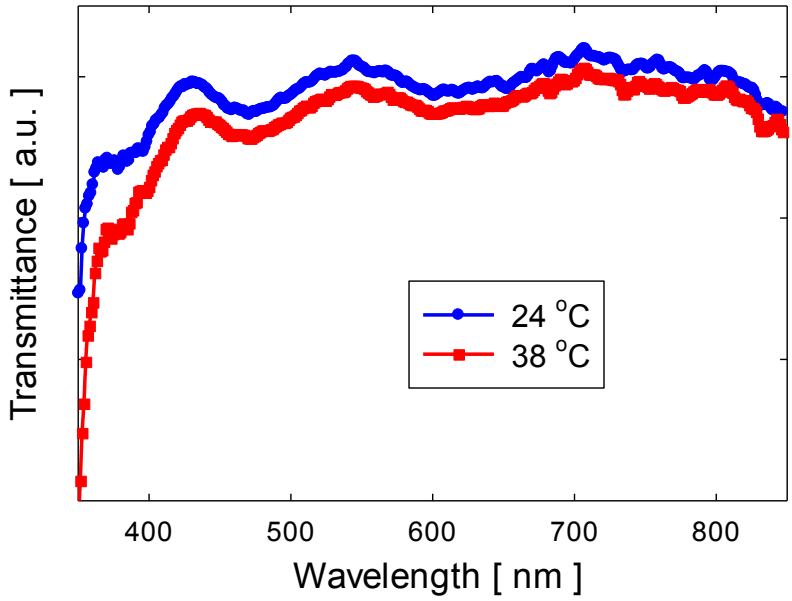

(e)

Figure 1. Song et al.

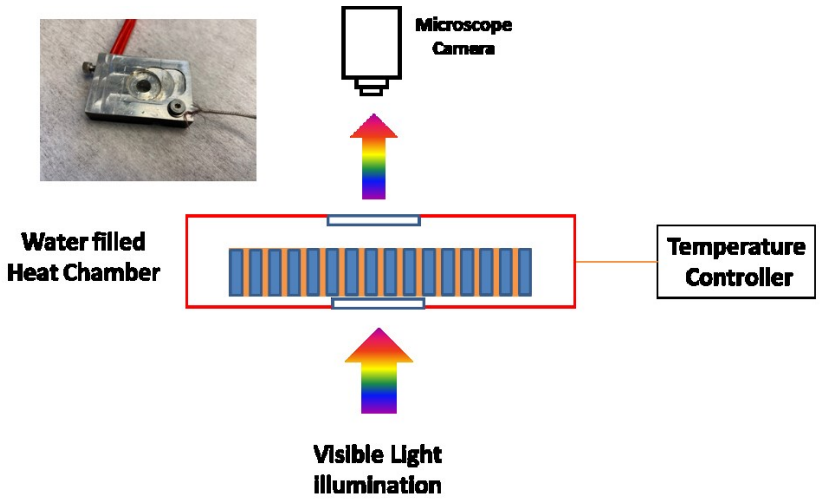

(a)

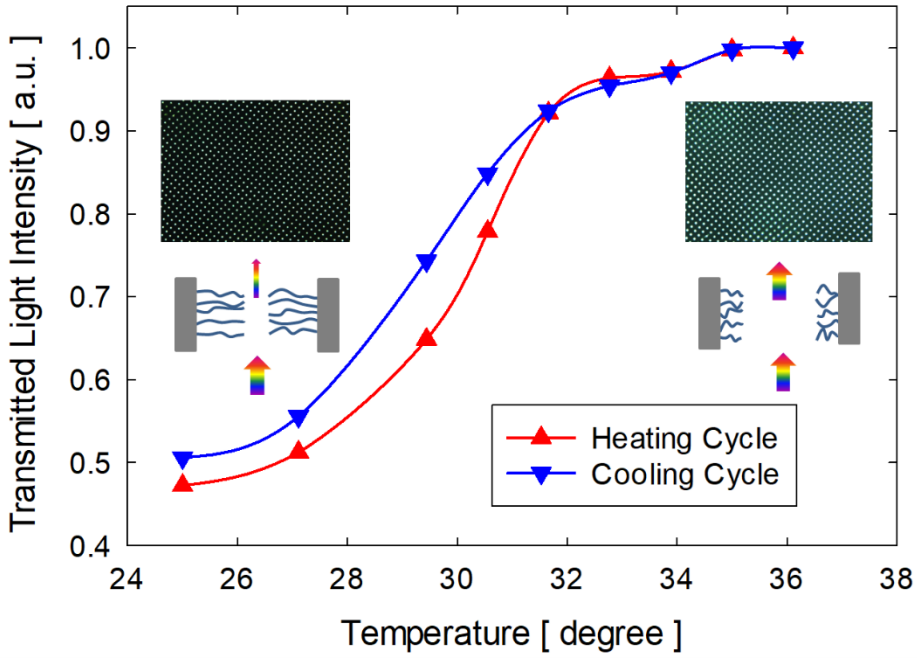

(b)

Figure 2. Song et al.

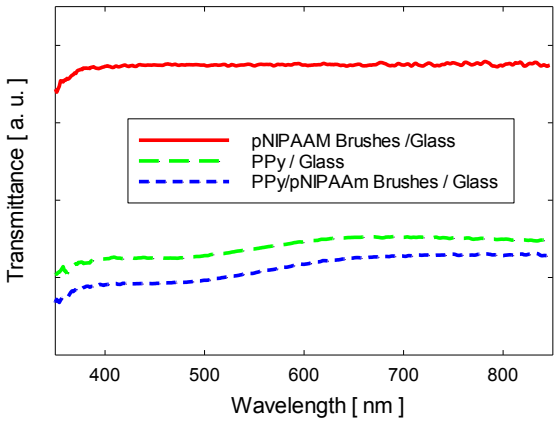

(a)

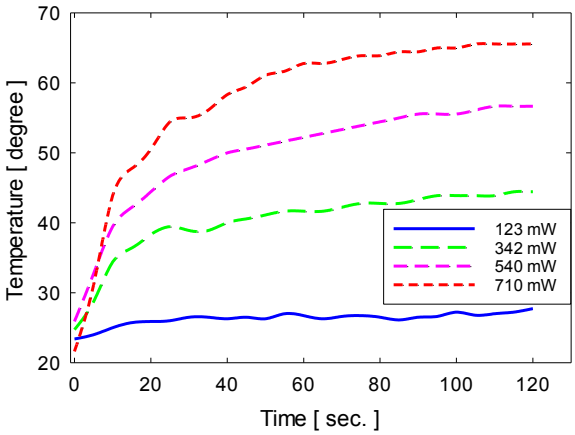

(b)

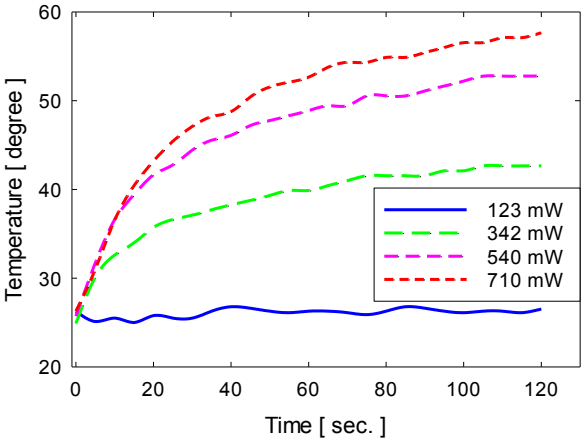

(c)

Figure 3. Song et al.

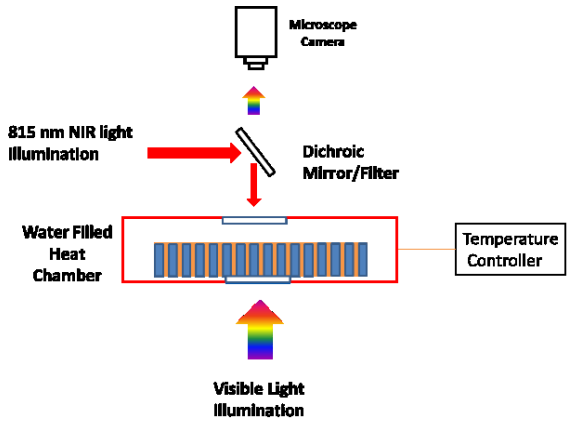

(a)

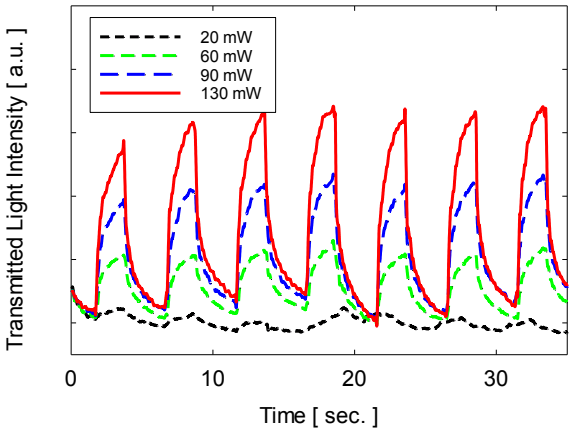

(b)

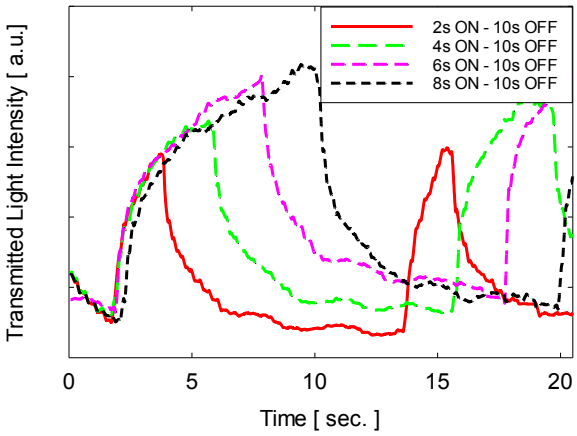

(c)

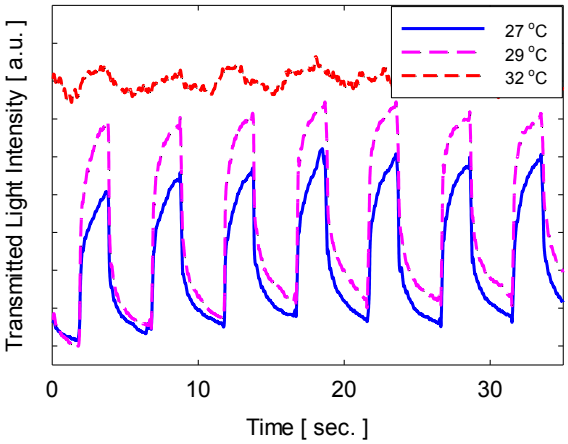

(d)

Figure 4. Song et al.

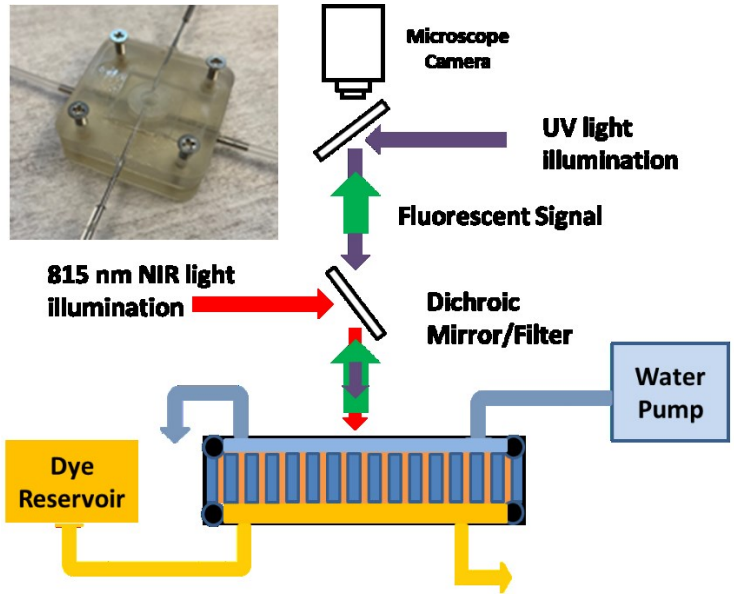

(a)

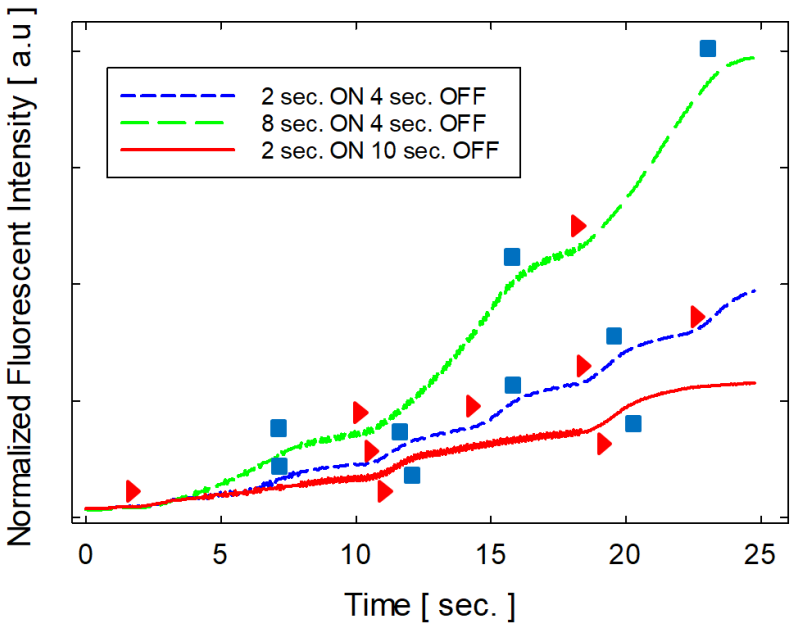

(b)

Figure 5. Song et al.

Supplementary Material

Video 1. Photothermal transient response of PPy/pNIPAAm brush layer along micron-sized pores in a macroporpus Si membrane with 130 mW NIR light power of pulsed (2 sec. ON and 3 sec. OFF) 815 nm NIR light illumination